



In vivo evidence of disseminated subpial T2* signal changes in multiple sclerosis at 7 T: A surface-based analysis

J. Cohen-Adad^{a,b}, T. Benner^{a,b}, D. Greve^{a,b}, R.P. Kinkel^{b,c}, A. Radding^{a,b}, B. Fischl^{a,b,d}, B.R. Rosen^{a,b}, C. Mainero^{a,b,*}

^a A.A. Martinos Center for Biomedical Imaging, Dept. of Radiology, Massachusetts General Hospital, Charlestown, MA, USA

^b Harvard Medical School, Boston, MA, USA

^c Beth Israel Deaconess Medical Center, Boston, MA, USA

^d CSAIL, MIT, Cambridge, MA, USA

ARTICLE INFO

Article history:

Received 17 December 2010

Revised 11 March 2011

Accepted 1 April 2011

Available online 13 April 2011

Keywords:

Multiple sclerosis

Subpial pathology

Ultra-high field MRI

T2*-weighted

Surface-based analysis

ABSTRACT

Cortical subpial demyelination is frequent in multiple sclerosis (MS) and is closely associated with disease progression and poor neurological outcome. Although cortical lesions have been difficult to detect using conventional MRI, preliminary data using T2*-weighted imaging at ultra-high field 7 T MRI showed improved sensitivity for detecting and categorizing different histological types of cortical MS lesions. In this study we combined high-resolution 7 T MRI with a surface-based analysis technique to quantify and map subpial T2*-weighted signal changes in seventeen patients with MS. We applied a robust method to register 7 T data with the reconstructed cortical surface of each individual and used a general linear model to assess *in vivo* an increase in subpial T2*-weighted signal in patients versus age-matched controls, and to investigate the spatial distribution of cortical subpial changes across the cortical ribbon. We also assessed the relationship between subpial T2* signal changes at 7 T, Expanded Disability Status Scale (EDSS) score and white matter lesion load (WMLL). Patients with MS showed significant T2*-weighted signal increase in the frontal lobes (parsopercularis, precentral gyrus, middle and superior frontal gyrus, orbitofrontal cortex), anterior cingulate, temporal (superior, middle and inferior temporal gyri), and parietal cortices (superior and inferior parietal cortex, precuneus), but also in occipital regions of the left hemisphere. We found significant correlations between subpial T2*-weighted signal and EDSS score in the precentral gyrus ($\rho = 0.56$, $P = 0.02$) and between T2*-weighted signal and WMLL in the lateral orbitofrontal, superior parietal, cuneus, precentral and superior frontal regions. Our data support the presence of disseminated subpial increases in T2* signal in subjects with MS, which may reflect the diffuse subpial pathology described in neuropathology.

© 2011 Elsevier Inc. All rights reserved.

Introduction

Post mortem examinations of MS brains consistently show that cortical subpial demyelination is frequent and extensive in multiple sclerosis (MS), and is closely associated with poor neurological outcome (Kutzelnigg and Lassmann, 2006; Magliozzi et al., 2007). The ability to detect and quantify subpial demyelination *in vivo* is needed to provide more definitive evidence of its role in the pathogenesis and evolution of MS.

While the contributions of both white matter (WM) macroscopic lesions and normal appearing WM (NAWM) damage to clinical outcome in patients with MS have been extensively studied by conventional and

non conventional MR techniques, the study of cortical subpial pathology in MS is constrained by the limitations of existing methods: histology can evaluate small cortical lesions and demyelination with great sensitivity, but is difficult to achieve for whole brain assessment; conventional MRI does not have the spatial resolution and contrast to detect and characterize the different types of cortical plaques described by neuropathology, including the important class of subpial lesions (Geurts et al., 2008; Kangarlu et al., 2007). Recent improvement in MR technology, using fluid-attenuated inversion recovery (FLAIR) and double-inversion recovery (DIR) imaging, has increased the potential to directly visualize cortical plaques in patients with MS, demonstrating that cortical lesions are a particularly good surrogate of clinical disability in MS (Calabrese et al., 2010; Pirko et al., 2007; Pulizzi et al., 2007; Sanfilippo et al., 2005; Tedeschi et al., 2005; Tjoa et al., 2005). The notion that gray matter (GM) involvement is a strong predictor of clinical status in MS is also supported by neuroimaging studies that assessed different aspects of cortical pathology including atrophy and magnetization transfer (Derakhshan et al., 2009; Stadelmann et al., 2008).

* Corresponding author at: A.A. Martinos Center for Biomedical Imaging, Massachusetts General Hospital, Building 149, Thirteenth Street, Charlestown, MA 02129, USA.

E-mail address: caterina@nmr.mgh.harvard.edu (C. Mainero).

Cortical lesions have been imaged with improved sensitivity *ex vivo* (Kangarlu et al., 2007; Pitt et al., 2010; Schmierer et al., 2010; Tardif et al., 2010) and *in vivo* (Kollia et al., 2009; Mainero et al., 2009) using ultra-high field systems (≥ 7 T), which, despite presenting some challenges related to B0 and B1 field inhomogeneities and higher energy deposition, show a great increase in signal-to-noise ratio (SNR) and consequently an increase in spatial resolution compared to 1.5 T–3 T MRI. The use of T2*-weighted images at 7 T also improves GM/WM contrast, allowing better identification of the lesion territory (Metcalf et al., 2010; Pitt et al., 2010). In addition, the combination of ultra-high field MRI with multichannel RF technology further increases the SNR, thus enabling an increase in spatial resolution, minimizing partial volume effects with adjacent cerebrospinal fluid (CSF) and WM. The advantages of 7 T and multichannel receive technology enabled us to identify in a small MS population different cortical lesion types, based on visual inspection of focal cortical hyperintensities on T2*-weighted fast low-angle shot (FLASH) and T2-weighted turbo spin echo images (Mainero et al., 2009). The frequency with which different lesion locations were observed in the cortical ribbon, including subpial lesions, conformed to recent neuropathology descriptions (Bø et al., 2003b). The number of subpial lesions correlated with clinical disease severity measures, suggesting that ultra-high field MRI is potentially a sensitive and specific marker of MS cortical pathology. Interestingly, T2*-weighted images were the most sensitive for detecting cortical MS lesions, compared to phase and T2-weighted images (Mainero et al., 2009). This finding has been corroborated by subsequent histopathological-MR correlations in post-mortem MS brains, which have highlighted the great sensitivity of T2*-weighted imaging to detect cortical MS pathology (Pitt et al., 2010).

Surface-based analysis methods provide a 2D parametric reconstruction of the cortex obtained from the segmentation of high resolution anatomical scans (Dale et al., 1999). This technique allows reconstruction of the pial surface and quantification of MRI signal at a given depth of the cortex (Fischl et al., 1999). Surface-based methods can therefore be used to quantify and assess the spatial distribution of subpial MR signal changes across different areas of the cortical mantle. Neuropathological examinations showed that in addition to manifesting as circumscribed, focal lesions, subpial demyelination may extend across multiple gyri leading to a phenomenon termed “general subpial demyelination” (Stadelmann et al., 2008). A surface-based approach has previously been used to measure cortical thinning in patients with MS compared to age-matched controls (Sailer et al., 2003).

In this study we combined *in vivo* measures of T2*-weighted signal at 7 T using a 32-channel RF coil with surface-based analysis of the whole brain cortex in 17 patients with MS. According to previous findings showing that cortical lesions appear as areas of hyperintensities on FLASH-T2* 7 T scans (Mainero et al., 2009; Metcalf et al., 2010; Pitt et al., 2010), we hypothesized that patients with MS would show a significant, diffuse subpial T2* signal increase versus age-matched controls. We also investigated the spatial distribution of subpial T2* signal changes across the cortex to test the hypothesis, supported by some neuropathological data, that cortical demyelinating changes, although disseminated, may show a preferential distribution across the cortical mantle and within cortical sulci and gyri (Bø et al., 2003b; Kutzelnigg and Lassmann, 2006). Finally, we assessed whether neurological disability as measured by the Expanded Disability Severity Scale (EDSS) and white matter lesion load (WMLL) is related to subpial T2* signal increases in specific cortical regions.

Material and methods

Subjects

Seventeen patients with clinically definite MS (Lublin and Reingold, 1996), (mean \pm SD age = 39.8 \pm 11.8 years; six males, eleven females), including ten patients with relapsing–remitting (RR) and seven with secondary progressive (SP) MS were included in the study along with

nine age-matched controls (five males, four females; mean \pm SD age = 34.7 \pm 10.8 years). All patients were clinically assessed within a week of the MRI using the Expanded Disability Status Scale (EDSS) (Kurtzke, 1983). Median EDSS was 3.5 and ranged from 1.0 to 6.5; mean \pm disease duration was 11.7 \pm 7.8 years.

Patients included in the study had to be relapse-free at least 3 months before study entry and without corticosteroid treatment for at least a month preceding study initiation. All patients except one had received disease-modifying agents for at least 3 months before the MRI. General exclusion criteria were significant medical, psychiatric, or neurologic history (other than MS for patients).

The local ethics committee of our Institution approved all experimental procedures of the study, and written informed consent was obtained from each study participant.

MRI acquisition

Subjects were scanned twice: 1) on a 7 T MRI (Siemens Medical Solutions) using a head gradient and 2) on a 3 T MRI (TIM Trio, Siemens Medical Solutions).

On the 7 T scanner we used an in-house single channel volume coil for RF transmission and an in-house 32-channel phased array coil for reception (Keil et al., 2010). Due to the tight fitting of the 32-channel coil and the large head size of some subjects, we used an in-house 8-channel phased array coil on 5 patients and one control. At the beginning of the session we performed manual B₀ shimming to minimize susceptibility effects. The imaging protocol included acquisition of T2*-weighted 2D Fast Low Angle Shot (FLASH) spoiled gradient-echo images with the following parameters: axial orientation, TR/TE = 1000/22 ms, flip angle = 55°, 2–3 slabs of 20 slices each to cover the supratentorial brain, FOV = 192 \times 168 mm², resolution = 0.33 \times 0.33 \times 1 mm³, bandwidth = 30 Hz/pix. The T2* slabs were acquired parallel to each other, with a 6-mm overlap to anticipate potential motion from the subject's head, thereby minimizing the chance of having a gap between slabs after registration to the structural image. We also acquired a T1-weighted 3D magnetization-prepared rapid acquisition gradient echo (MPRAGE) with the following parameters: axial orientation, TR/TI/TE = 2600/1100/3.26 ms, flip angle = 9°, FOV = 194 \times 192 mm², resolution = 0.6 \times 0.6 \times 1.5 mm³, bandwidth = 200 Hz/pix.

On the 3 T scanner we used the body coil for RF excitation and the commercially-available 32-channel coil (Wiggins et al., 2006) for signal reception. The protocol included a high-resolution structural 3D scan with a magnetization-prepared rapid acquisition with multiple gradient echoes (MEMPR) (van der Kouwe et al., 2008) sequence (TR/TI = 2530/1200 ms, TE = [1.7; 3.6; 5.4; 7.3] ms, flip angle = 7°, FOV = 230 \times 230 mm², resolution = 0.9 \times 0.9 \times 0.9 mm³, bandwidth = 651 Hz/pix). The root mean square (RMS) average of all echoes of the 3 T MEMPR data was used to reconstruct the cortical surface models of each individual. We found this procedure to be more robust when using the 3 T rather than the 7 T MPRAGE image – notably due to the difficulty of having homogeneous B₁ field at 7 T.

Processing

Fig. 1 shows the processing pipeline. Cortical surface was reconstructed in each subject on 3 T MEMPR images using FreeSurfer software (<http://surfer.nmr.mgh.harvard.edu/>). 7 T data were then registered on each individual surface, mapped at a given depth from the pial surface and analyzed using a general linear model (GLM) framework to test for significant T2* signal change between MS patients and controls. Accurate segmentation of the WM/GM interface was sometimes hampered by the presence of hypointense leukocortical lesions on the T1-weighted multiecho MPRAGE images. Hence, we visually checked all subjects (patients and controls) and manually adjusted the reconstructed surface on the FreeSurfer editing tools when needed. Editing included both manual adjustment of the surface

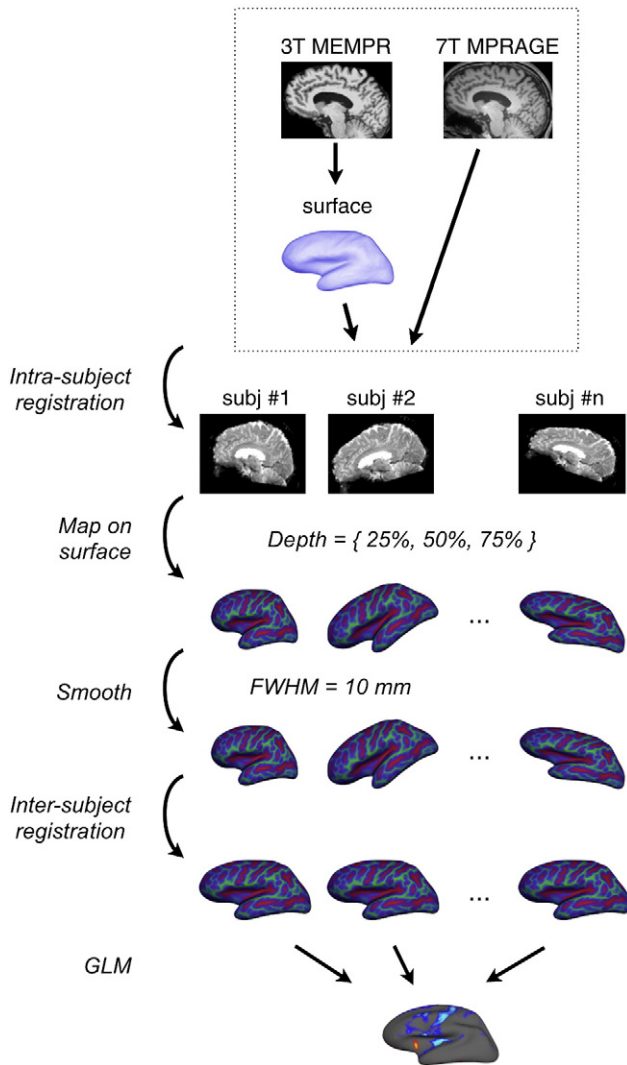


Fig. 1. Processing pipeline for surface-based analysis applied to 7 T images. Dashed box concerns intra-subject registration and is further detailed on Fig. 2.

and automated intensity correction (control points) of the leukocortical lesions included in the cortical surfaces.

Registration

Registration of 7 T scans to the 3 T MEMPR was performed using a two-step procedure: 1) within-subject registration of 7 T images to the 3 T surface and 2) between-subject normalization of each 7 T FLASH scan to a surface template.

Fig. 2 shows the pipeline of the within-subject registration. First, the 7 T MPRAGE and 3 T MEMPR were corrected for intensity non-uniformity (Sled et al., 1998). Then, the 7 T MPRAGE was registered to the 3 T MEMPR using FSL FLIRT (<http://www.fmrib.ox.ac.uk/fsl/>) (rigid-body transformation with 6 degrees of freedom and mutual information as cost function). An initial registration between each 7 T FLASH slab and the 7 T MPRAGE was then computed from the geometry information in the DICOM header (pre-alignment). If subject moved within the same session, a manual registration was performed using FreeSurfer interface (gross alignment). Next, a fine alignment was produced using a new boundary-based registration (BBR) method (Greve and Fischl, 2009) (rigid-body transformation with 6 degrees of freedom). This type of registration is based on the intensity gradient across tissue boundaries and was preferred to a more classical volume-based method due to the low information overlap between the full brain 7 T MPRAGE and one single slab from the 7 T FLASH scan. Visual inspection was systematically

conducted to assess proper registration. BBR has been shown to be more accurate and robust than other commonly used registration procedures (Greve and Fischl, 2009). Following registration, individual slabs were combined using FreeSurfer tools to generate a FLASH-T2* volume containing the full supratentorial brain. The volume was then corrected for intensity non-uniformity (Sled et al., 1998) (number of iterations = 2, number of protocol iterations = 40).

Mapping of MRI signal

Given that cortical thickness varies by a substantial amount throughout the cortex, depth was not defined as an absolute distance from the pial surface, but rather as a relative distance between the pial and the white matter surface. This approach ensured better conservation of a layer-specific mapping, which is desirable when addressing neuropathological hypotheses related to the distribution of subpial lesions. MRI signal was therefore sampled along the midline of the cortical ribbon.

Surface-based smoothing

Following surface mapping, signal was smoothed along the surface using a 2D smoothing approach. 2D smoothing offers the advantage of averaging locations along the folding pattern of the cortex, therefore minimizing partial volume effects with neighboring structure (e.g., CSF, white matter). Based on visual inspection, subpial demyelinating lesions could extend across multiple gyri (i.e., several centimeters) and could also manifest as focal small lesions (~2–3 mm). To be sensitive to the two manifestations of subpial demyelination, smoothing was performed using a 10 mm full width at half maximum (FWHM) Gaussian kernel. Subject’s motion between acquisitions of FLASH slabs may have introduced a narrow space of null signal between the registered slabs. Smoothing over the whole surface would have drastically decreased the mean signal at the border of these null vertices. To avoid this situation, a mask was generated from the T2* surface (before smoothing) to exclude those vertices from the smoothing procedure and from the rest of the analysis.

Group analysis

All subjects were registered to a surface template ‘fsaverage’ using FreeSurfer. A general linear model (GLM) was performed to test subpial T2* signal differences between controls and patients across the whole cortex. The GLM was run on a vertex-by-vertex basis after normalizing each individual surface by its mean signal. Regions of significant signal change were identified using the cortical atlas provided by FreeSurfer (Desikan et al., 2006).

Using the FreeSurfer masks of gyri and sulci, we quantitatively assessed whether subpial T2* hyperintensity is preferential distributed within gyri or sulci. In each mask we computed the number of vertices exhibiting significant change (p < 0.05). For comparison, this number was normalized by the total number of vertices in gyri (N = 166763) and sulci (N = 160921).

Correlation with WMLL and EDSS

WMLL was calculated on FLASH-T2* images as previously described (Mainero et al., 2001) using the software Alice (Hayden Image Processing Solutions) based on a local threshold contouring technique of white matter hyperintensities. WMLL median (min–max) was 2614.78 (63.7–12439.92) mm³. Spearman’s correlation between subpial T2*-weighted signal and WMLL was computed on a vertex-by-vertex basis for all patients (N = 17) using the FLASH-T2* images normalized by their mean signal (as for the GLM analysis).

Spearman’s correlation was also computed between EDSS score and the normalized T2*-weighted signal averaged within the pre-central gyrus, given that EDSS score is mostly weighted towards motor impairment.

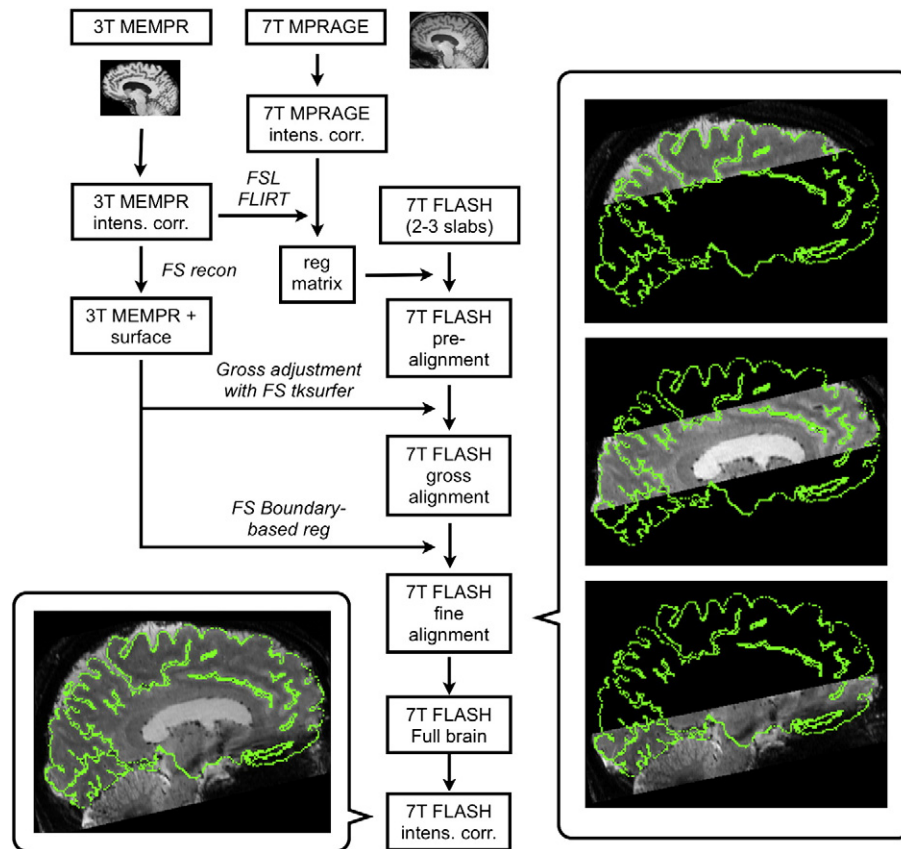


Fig. 2. Processing pipeline for intra-subject registration (dashed box in Fig. 1). Following intensity inhomogeneity correction (intens. corr.), the 7 T MPRAGE was registered on the 3 T MEMPR using FSL FLIRT. An initial registration between each 7 T slab and the 7 T MPRAGE was then computed from the geometry information in the DICOM header (pre-alignment). A manual registration was then performed using FreeSurfer interface (gross alignment). Next, a fine alignment was produced using FreeSurfer boundary-based registration. Following registration, all individual slabs were concatenated to generate a volume containing the full supratentorial brain. The volume was then corrected for intensity non-uniformity.

Results

High spatial resolution combined with high contrast enabled the detection of white and gray matter pathology. The amount of artifacts was relatively minimal: one subject exhibited slight motion artifacts (blurring), and one subject exhibited Eddy-current artifacts. Susceptibility artifacts were noticeable in all subjects (patients and controls) in the sinus area, yielding slight signal decrease in the posterior part of the lower brain. Manual registration (gross alignment) was performed on about 90% of the subjects to ensure maximal robustness of fine registration on surfaces. However, since the pre-registration was relatively accurate (i.e., 7 T MPRAGE on the 3 T MEMPRAGE using FSL FLIRT), less than one minute per slab was required to slightly adjust each slab to the surface. Visual inspection confirmed that all 7 T images were successfully registered to the surface. Fig. 3A shows an axial view of a FLASH image from an SPMS patient. A zoomed panel focuses on a cortical lesion (arrow) and shows the result of segmentation with delineation of the pial surface (red) and GM/WM boundary (yellow). Surface mapping yielded relatively homogeneous signal for healthy subjects and visible hyperintensities in MS patients. Fig. 3B shows an example of T2*-weighted signal mapped at 50% depth for a control (left) and another SPMS patient (right) where lesions appear as hyperintensities (arrows).

The GLM analysis detected significant differences between control and MS patients (Fig. 4). Overall, patients showed increased subpial T2* signal compared to controls in several areas of the frontal, temporal and parietal lobes of both hemispheres (Table 1). Changes were also detected in occipital areas, mostly on the left hemisphere. We tested the effect of gender on our MR measures by adding a regressor on the GLM analysis. Results showed no significant effect of the gender regressor throughout the cortex ($P < 0.05$, uncorrected).

We also tested the effect of using the 8-channel coil versus the 32-channel coil, by excluding subjects scanned with the 8-channel coil. Despite slight differences between the two analyses – that could be accounted by different population size, results produced with or without the 8-channel coil were very similar.

The total area of hyperintensities in cortical gyri was two times greater than that in sulci when comparing MS patients versus controls: the number of vertices (normalized by the total number of vertices) exhibiting significant signal changes was 0.0367 in sulci and 0.0679 in gyri.

Fig. 5 shows Spearman's correlations (thresholded at $P = 0.05$) between subpial T2* signal and white matter lesion load. Significant positive correlations were detected in the lateral orbitofrontal, superior parietal, cuneus, precentral and superior frontal regions. Very few negative correlations were detected and were localized in the right middle temporal and the left lingual areas.

Fig. 6 shows correlation between EDSS score and T2*-weighted signal averaged in the precentral gyrus was also significant ($\rho = 0.56$, $P = 0.02$), suggesting a relationship between T2* hyperintensities caused by GM pathology in the primary motor cortex and motor deficits.

Discussion

Surface-based analysis from 7 T data in patients with MS revealed a significant T2*-weighted signal increase in several regions of the cortex, which may reflect the diffuse subpial pathology described in autopsy cases of MS (Bø et al., 2003b; Kidd et al., 1999; Kutzelnigg and Lassmann, 2006; Pitt et al., 2010; Schmierer et al., 2010; Stadelmann et al., 2008). The proposed method facilitates the characterization of cortical MS lesions *in vivo* by allowing accurate quantification of subpial signal changes across populations, and their spatial distribution, unbiased by

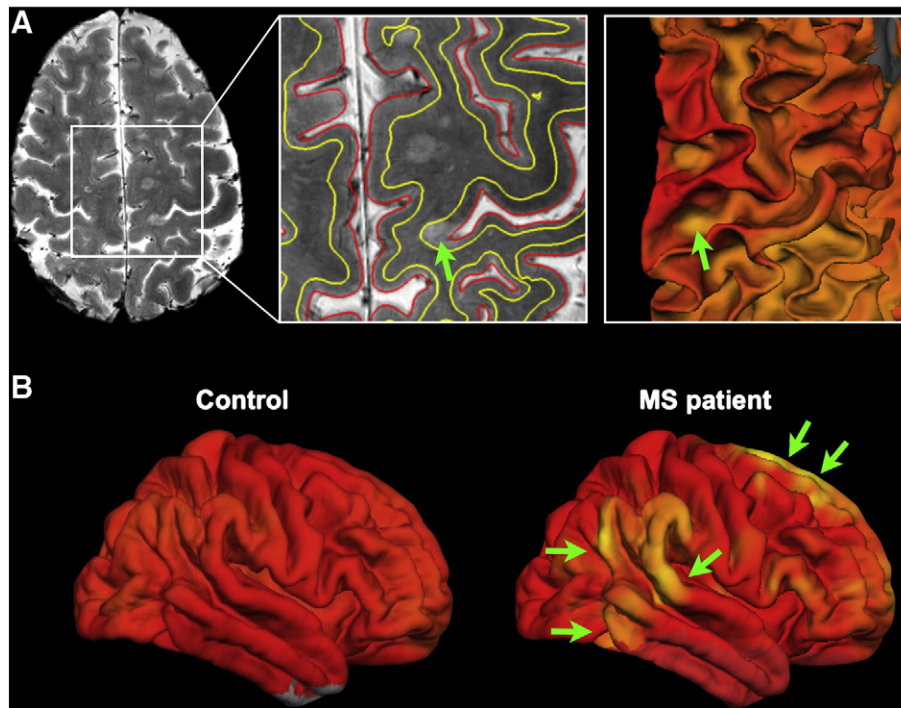


Fig. 3. A. 7 T FLASH image of a patient with SPMS. Zoomed panel shows an overlay of pial (red) and white matter surfaces (yellow). The right zoomed panel shows the reconstructed white matter surface of the same patient with T2*-weighted signal mapped on the surface. Cortical pathology is visible on both the T2*-weighted volume and on the surface (green arrow). B. Mapping of T2*-weighted signal on the common surface space (fsaverage) for a control (left) and another SPMS patient (right). Diffuse hyperintensities are observed in the MS patient (arrows).

evaluations based on visual inspection of scans. It also allows examining the entire cortical ribbon, which is technically difficult to achieve in histopathology studies.

The combination of 7 T imaging with multichannel RF technology enabled us to trade off the resultant high SNR for very small voxel volumes (0.1 mm³), necessary to explore various depths of the cortical ribbon and to reduce partial volume effects, especially with adjacent CSF and WM.

Technical challenges

Due to SAR limitation and SNR consideration, we constrained our slice thickness to 1 mm, whereas in-plane resolution was 0.3 × 0.3 mm². Hence, depending on the orientation of the cortical ribbon, it is possible that the sensitivity to detect changes may be lower in regions where the

cortical surface is somewhat aligned with the slice due to partial volume effect in the slice direction.

Another challenge at 7 T is that B1 field is highly inhomogeneity and may have led to variable regional sensitivity. To minimize the inter-subject variability, a B1-map was acquired after manual shimming and before acquiring the T2* slabs. Based on the B1-map, we estimated the voltage to target a specific flip angle. To correct for intra-subject B1-inhomogeneities, we applied an intensity inhomogeneity correction algorithm, as has been described in the methods (Sled et al., 1998). Since this algorithm alters the global signal intensity, we normalized the T2*-weighted signal by the mean value across the cortex before further processing. This procedure minimized regional variabilities of T2*-weighted signal for the GLM and for the correlation analysis. One way to overcome the B1-inhomogeneity

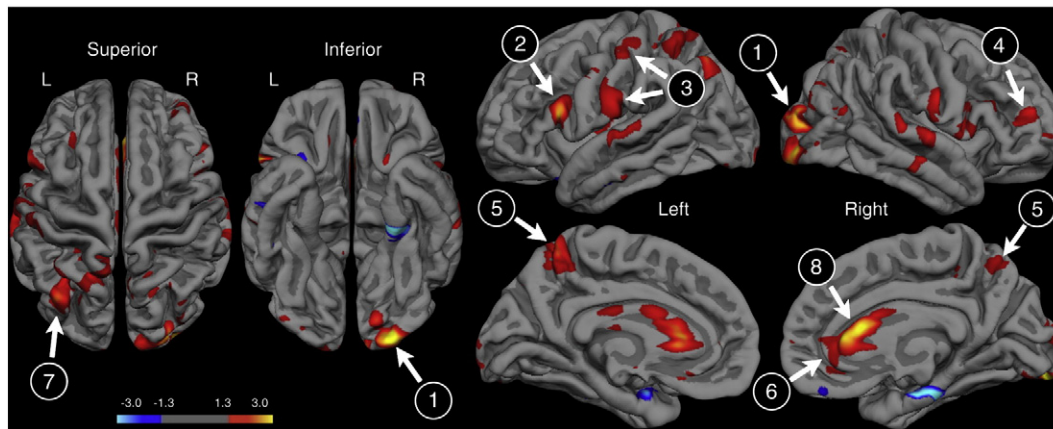


Fig. 4. Overlay of the GLM significance maps ($-\log_{10}(P)$) on the average pial surface for all patients (N = 17) versus controls (N = 9). Most significant changes in T2*-weighted signal occur in the lateral occipital (1), left parsopercularis (2), sensorimotor region (3), middle frontal (4), precuneus (5), anterior cingulate (6), superior parietal (7). Although the focus here was to study the gray matter, T2*-weighted signal was also mapped around the ventricles, including the corpus callosum (8). Regions were identified using the Freesurfer cortical labeling atlas.

Table 1
Brain cortical areas showing significantly increased subpial T2* signal in 17 patients with multiple sclerosis compared to nine age-matched controls.

Location	Left hemisphere		Right hemisphere	
	Peak T		Peak T	
Superior frontal	3.42			
Middle frontal	3.49		3.58	
Medial orbitofrontal	3.34		2.58	
Lateral orbitofrontal	3.44		2.57	
Anterior cingulate	3.54		2.56	
Pars triangularis	3.41		2.51	
Pars opercularis	3.44		2.66	
Paracentral	3.33		–	
Precentral	3.36		2.54	
Postcentral	3.49		2.59	
Superior temporal	3.46		2.60	
Middle temporal	3.51		2.58	
Inferior temporal	3.43		–	
Superior Parietal	3.38		2.60	
Inferior parietal	–		2.64	
Precuneus	3.34		2.61	
Cuneus	3.38		–	
Pericalcarine	3.46		–	
Lingual	3.53		–	
Lateral occipital	3.58		2.59	

R = right; L = left; T = P < 0.05.

issue would be to acquire multiecho T2*-weighted data and estimate the T2* value.

Source of T2* signal change

In the present study we mostly detected a positive subpial T2*-weighted signal change in MS patients compared to age-matched controls. Although previous MR studies suggested that T2-hyperintense lesions are nonspecific for the underlying pathology and may include varying degrees of inflammation, demyelination, gliosis, edema, degenerative phenomena secondary to local discrete areas of demyelination, and retrograde and trans-synaptic degeneration of fibers passing through WM plaques (Filippi and Rocca, 2010; Lassmann, 2008; Neema et al., 2007b; Stadelmann et al., 2008), it is well documented that cortical lesions have a lesser inflammatory component than WM lesions, therefore contain fewer iron-rich macrophages (Bø et al., 2003a). Recent ultra-high field studies of post mortem MS brains reported a significant negative correlation between T2 and myelin concentration in the cortex (Schmierer et al., 2010), thereby suggesting that hyperintensities detected in the present study are associated with general demyelination. In addition, recent histopathological-MR correlations at 7T MRI in post-mortem MS brains, showed that the majority of cortical lesions appears as areas of increased T2*-weighted signal (Pitt et al., 2010).

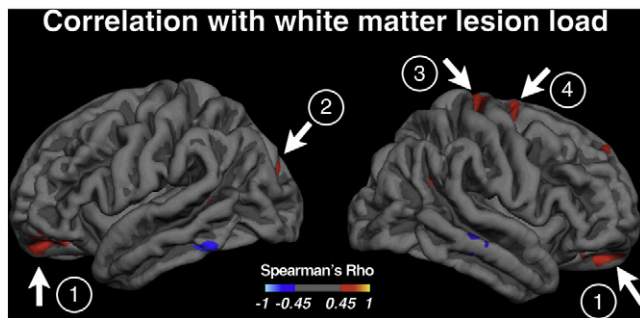


Fig. 5. Spearman's correlation coefficient between T2* signal and white matter lesion load. Results are slightly smoothed (FWHM = 3 mm) and thresholded (P < 0.05). Significant correlations are detected in the lateral orbitofrontal (1), cuneus (2), precentral (3) and superior frontal (4) areas.

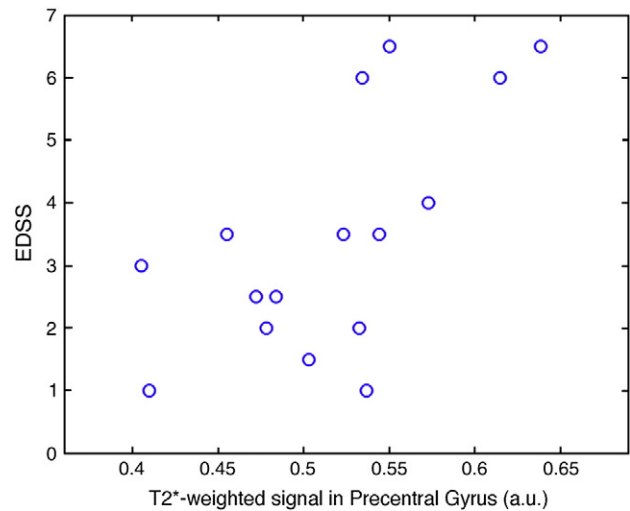


Fig. 6. Spearman's correlation between EDSS score and T2*-weighted signal averaged in the precentral gyrus ($\rho = 0.56$, $P = 0.02$). For this analysis one subject was removed because part of his precentral gyrus was out of the field of view.

Our data showed that only a small portion of the brain was affected by negative signal change. T2- and T2*-hypointense lesions have been associated with increase in iron content associated with neurodegeneration and inflammation (Filippi and Rocca, 2010; Neema et al., 2007a; Pitt et al., 2010). Our previous data at 7 T, however, showed that cortical lesions are difficult to detect using phase data (Mainero et al., 2009).

Given that subpial demyelination is likely a T2 effect, one could argue that the benefits of using ultra-high field MRI for detecting cortical pathology in MS are not as strong as if it would be a susceptibility effect. There is, however, an advantage for using 7T scanners thanks to a substantial increase in signal-to-noise ratio and consequently an increase in the achievable spatial resolution.

Distribution of lesions throughout the cortex

Post mortem examinations of MS brains suggest that all brain lobes can be similarly affected by cortical lesions, although some pathological findings report that cortical demyelination may be preferentially-distributed, with demyelinating processes occurring preferentially in the cingulate gyrus, the insula and the temporobasal cortex (Bø et al., 2003b; Kutzelnigg and Lassmann, 2006). In previous *in vivo* studies cortical lesions were mostly detected in the frontal cortex (Bagnato et al., 2006) as well as in temporal, parietal and less commonly observed in occipital regions (Mainero et al., 2009). The present study supports a diffuse distribution of lesions in specific areas of the frontal lobe (parsopercularis, precentral gyrus, middle and superior frontal gyrus, orbitofrontal cortex), anterior cingulate, temporal (superior, middle and inferior temporal gyri), and parietal cortices (superior and inferior parietal cortex, precuneus), but also occipital regions mainly in the left hemisphere. Higher density of demyelinating processes around veins may partially explain this distribution across the cortex (Kidd et al., 1999). Previous studies reported that subpial demyelination might extend over multiple gyri leading to a phenomenon termed the “general subpial demyelination”. Other pathological findings described cortical sulci as being preferentially affected by subpial demyelination, underlying the hypothesis that stagnant CSF may induce or predispose subpial demyelination (Peterson et al., 2001). Here, we found that both gyri and sulci were affected by significant T2* signal increases in MS patients compared to controls; however cortical gyri exhibited a larger area of subpial hyperintensity than sulci.

Specificity to lesion type

Subpial demyelination may manifest as focal or more diffuse lesions across multiple gyri (Stadelmann et al., 2008). Here, we used a GLM to test regional signal change between patients and controls. This method is more sensitive to signal intensity changes that appear at higher rate and/or that are similarly distributed across an MS population. If subpial changes were randomly distributed, then our method wouldn't optimally detect them – because of an averaging effect across the population. Therefore in this study we quantified the overall load of subpial intensity changes, which likely included both focal and diffuse pathology. In our previous visual observations of FLASH T2* scans in patients with MS, we found that lesions that extend partially or completely throughout the cortical depth (type III/IV) had the highest incidence. These lesions were preferentially distributed in cortical areas similar to those observed in the present study. Furthermore, pathological data have shown that most subpial lesions affect the outer three or four layers of the cortex but in the largest lesions the entire cortical ribbon was demyelinated (Kutzelnigg and Lassmann, 2006). Other authors that have measured magnetization transfer ratio (MTR) in the cortex of MS patients have shown that larger MTR changes occur in the superficial layer of the cortex (Derakhshan et al., 2009).

Impact of cortical atrophy

Cortical atrophy is known to occur in MS and may be associated with T2* signal increase. We recently showed a strong relation between cortical thinning and the overall number of subpial (type III/IV) cortical lesions, but no association with the overall number of leukocortical lesions (Mainero et al., 2010). The spatial distribution of cortical thinning partly, but not completely, overlap with the distribution of diffuse subpial signal T2* changes at 7T, and with correlation maps between the number of type III/IV lesions and cortical thickness across both hemispheres. Although these findings need to be confirmed in a larger MS population, they do suggest that subpial lesions and cortical atrophy may not necessarily share a “cause–effect” relationship but reflect two different aspects of the same degenerative process.

Correlation with WMFL and disability

In this study we mostly found positive correlations between WMFL and T2*-weighted signal in the lateral orbitofrontal, superior parietal, cuneus, precentral and superior frontal regions. These cortical regions also showed increased T2* signal in patients relative to controls. Although we did not include measurements of NAWM involvement, our finding might either reflect a true interdependence or a stage dependent common pathogenic pathway for WM and cortical tissue injury. Longitudinal evaluations, as well as assessment of damage along specific WM tracts with diffusion imaging tractography can be used in future studies to investigate this aspect of MS pathology.

Significant correlation was also detected between EDSS score and T2*-weighted signal averaged in the primary motor cortex (precentral gyri). This finding represents a major step forward from our previous observation of a positive correlation between EDSS and the overall number of subpial lesions in subjects with MS (Mainero et al., 2009). Other studies also reported correlations between EDSS, intracortical T2 lesion load (Calabrese et al., 2007; Fisniku et al., 2008; Li et al., 2006; Mainero et al., 2009), and reduced MTR in the right primary motor cortex (Khaleeli et al., 2007).

Several studies have reported a strong relationship between neocortical atrophy and clinical status (EDSS and disease duration) (De Stefano et al., 2003; Sanfilippo et al., 2005). Although GM atrophy and lesion load are known to be good predictors of clinical disability and clinical outcome (Charil et al., 2007; Khaleeli et al., 2008), the causal relationship between these two surrogate markers is still uncertain

(Chard and Miller, 2009; Miller et al., 2002). Mapping the topography of cortical lesions and atrophy across time could potentially provide new insights into the interaction of these two markers (Mainero et al., 2010). Furthermore, the use of more sensitive clinical markers of disease status and outcome including neuropsychological assessments can provide increased specificity and sensitivity of cortical regional and global involvement than EDSS, which is known to be heavily weighted towards motor disability.

Conclusion

This study demonstrates the feasibility of surface-based analysis of T2*-weighted signal from 7T acquisition with a highly parallelized RF coil. Applying this technique in MS patients and age-matched controls, we detected an overall signal increase in specific areas of the cortex in patients, providing evidence for the *in vivo* existence of distributed subpial changes in MS. Our surface-based analysis of subpial T2* signal allowed us to quantify and spatially characterize GM cortical pathology via an accurate mapping of the neocortex across a population of subjects with MS, and potentially across different disease phenotypes. This method could therefore be valuable for understanding the pathogenesis of MS cortical lesions, and for monitoring the effect of new treatments (Chard and Miller, 2009). Other metrics sensitive to MS GM pathology can be combined with a similar surface-based approach to further investigate the nature of cortical changes *in vivo*. These include: T1, T2 or T2* mapping (Hammond et al., 2008; Tardif et al., 2010), MTR (Derakhshan et al., 2009), and fractional anisotropy measures derived from diffusion tensor imaging (Poonawalla et al., 2008). Computational methods also provide a means to quantify MR signal in deep gray matter structures. Given that deep nuclei in MS are known to be affected by GM demyelination (Pirko et al., 2007), mapping MR signal change in deeper sub-cortical structures such as in the basal ganglia and the thalamus may help understanding how abnormalities in these structures (e.g. iron deposit and neurodegenerative processes) are associated with MS outcome.

Acknowledgments

We thank Dr Andre van der Kouwe for his technical help, Drs Larry Wald and Boris Keil for helping with the 7 T coil and Drs Rikke Jensen and Scott Nielsen for helping with patients recruitment and. This work was partly supported by a grant of the National Multiple Sclerosis Society [4281-RG-A-1 to C.M.], and by the National Center for Research Resources [P41-RR14075, and the NCRB BIRN Morphometric, Project BIRN002, U24 RR021382]. **J.C-A was supported by a fellowship from the Association pour la Recherche sur la Sclérose en Plaques (ARSEP, France), B.F. was supported by the National Institute for Biomedical Imaging and Bioengineering [R01EB006758], the National Institute on Aging [AG022381], the National Institute for Neurological Disorders and Stroke [R01 NS052585-01], the Mental Illness and Neuroscience Discovery [MIND] Institute, the National Alliance for Medical Image Computing [NAMIC], the National Institutes of Health through the NIH Roadmap for Medical Research, Grant U54 EB005149 and the Autism & Dyslexia Project funded by the Ellison Medical Foundation.

References

- Bagnato, F., Butman, J.A., Gupta, S., Calabrese, M., Pezawas, L., Ohayon, J.M., Tovar-Moll, F., Riva, M., Cao, M.M., Talagala, S.L., McFarland, H.F., 2006. *In vivo* detection of cortical plaques by MR imaging in patients with multiple sclerosis. *AJNR. Am. J. Neuroradiol.* 27, 2161–2167.
- Bø, L., Vedeler, C.A., Nyland, H., Trapp, B.D., Mørk, S.J., 2003a. Intracortical multiple sclerosis lesions are not associated with increased lymphocyte infiltration. *Mult. Scler.* 9, 323–331.
- Bø, L., Vedeler, C.A., Nyland, H.I., Trapp, B.D., Mørk, S.J., 2003b. Subpial demyelination in the cerebral cortex of multiple sclerosis patients. *J. Neuropathol. Exp. Neurol.* 62, 723–732.
- Calabrese, M., de Stefano, N., Atzori, M., Bernardi, V., Mattisi, I., Barachino, L., Morra, A., Rinaldi, L., Romualdi, C., Perini, P., Battistin, L., Gallo, P., 2007. Detection of cortical

- inflammatory lesions by double inversion recovery magnetic resonance imaging in patients with multiple sclerosis. *Arch. Neurol.* 64, 1416–1422.
- Calabrese, M., Filippi, M., Gallo, P., 2010. Cortical lesions in multiple sclerosis. *Nat. Rev. Neurol.* 6, 438–444.
- Chard, D., Miller, D., 2009. Grey matter pathology in clinically early multiple sclerosis: evidence from magnetic resonance imaging. *J. Neurol. Sci.* 282, 5–11.
- Charil, A., Dagher, A., Lerch, J.P., Zijdenbos, A.P., Worsley, K.J., Evans, A.C., 2007. Focal cortical atrophy in multiple sclerosis: relation to lesion load and disability. *Neuroimage* 34, 509–517.
- Dale, A.M., Fischl, B., Sereno, M.I., 1999. Cortical surface-based analysis. I. Segmentation and surface reconstruction. *Neuroimage* 9, 179–194.
- De Stefano, N., Matthews, P.M., Filippi, M., Agosta, F., De Luca, M., Bartolozzi, M.L., Guidi, L., Ghezzi, A., Montanari, E., Cifelli, A., Federico, A., Smith, S.M., 2003. Evidence of early cortical atrophy in MS: relevance to white matter changes and disability. *Neurology* 60, 1157–1162.
- Derakhshan, M., Caramanos, Z., Narayanan, S., Collins, D., Arnold, D., 2009. Regions of reduced cortical magnetization transfer ratio detected in MS patients using surface-based techniques. Proceedings of the 17th Annual Meeting of ISMRM, Honolulu, USA, p. 338.
- Desikan, R.S., Ségonne, F., Fischl, B., Quinn, B.T., Dickerson, B.C., Blacker, D., Buckner, R.L., Dale, A.M., Maguire, R.P., Hyman, B.T., Albert, M.S., Killiany, R.J., 2006. An automated labeling system for subdividing the human cerebral cortex on MRI scans into gyral based regions of interest. *Neuroimage* 31, 968–980.
- Filippi, M., Rocca, M.A., 2010. MR Imaging of Gray Matter Involvement in Multiple Sclerosis: Implications for Understanding Disease Pathophysiology and Monitoring Treatment Efficacy. *AJNR Am. J. Neuroradiol.* 31 (7), 1171–1177.
- Fischl, B., Sereno, M.I., Dale, A.M., 1999. Cortical surface-based analysis. II: Inflation, flattening, and a surface-based coordinate system. *Neuroimage* 9, 195–207.
- Fisniku, L.K., Brex, P.A., Altmann, D.R., Miszkiewicz, K.A., Benton, C.E., Lanyon, R., Thompson, A.J., Miller, D.H., 2008. Disability and T2 MRI lesions: a 20-year follow-up of patients with relapse onset of multiple sclerosis. *Brain* 131, 808–817.
- Geurts, J.J., Blezer, E.L., Vrenken, H., van der Toorn, A., Castelijns, J.A., Polman, C.H., Pouwels, P.J., Bo, L., Barkhof, F., 2008. Does high-field MR imaging improve cortical lesion detection in multiple sclerosis? *J. Neurol.* 255, 183–191.
- Greve, D.N., Fischl, B., 2009. Accurate and robust brain image alignment using boundary-based registration. *Neuroimage* 48, 63–72.
- Hammond, K.E., Lupo, J.M., Xu, D., Metcalf, M., Kelley, D.A., Pelletier, D., Chang, S.M., Mukherjee, P., Vigneron, D.B., Nelson, S.J., 2008. Development of a robust method for generating 7.0 T multichannel phase images of the brain with application to normal volunteers and patients with neurological diseases. *Neuroimage* 39, 1682–1692.
- Kangarlu, A., Bourekas, E.C., Ray-Chaudhury, A., Rammohan, K.W., 2007. Cerebral cortical lesions in multiple sclerosis detected by MR imaging at 8 Tesla. *AJNR. Am. J. Neuroradiol.* 28, 262–266.
- Keil, B., Triantafyllou, C., Hamm, M., Wald, L.L., 2010. Design optimization of a 32-channel head coil at 7 T. Proceedings of the 18th Annual Meeting of ISMRM, Stockholm, Sweden, 1493.
- Khaleeli, Z., Cercignani, M., Audoin, B., Ciccarelli, O., Miller, D.H., Thompson, A.J., 2007. Localized grey matter damage in early primary progressive multiple sclerosis contributes to disability. *Neuroimage* 37, 253–261.
- Khaleeli, Z., Altmann, D., Cercignani, M., Ciccarelli, O., Miller, D., Thompson, A., 2008. Magnetization transfer ratio in gray matter: a potential surrogate marker for progression in early primary progressive multiple sclerosis. *Arch. Neurol.* 65, 1454.
- Kidd, D., Barkhof, F., McConnell, R., Algra, P.R., Allen, I.V., Revesz, T., 1999. Cortical lesions in multiple sclerosis. *Brain* 122 (Pt 1), 17–26.
- Kollia, K., Maderwald, S., Putzki, N., Schlamann, M., Theysohn, J.M., Kraff, O., Ladd, M.E., Forsting, M., Wanke, I., 2009. First clinical study on ultra-high-field MR imaging in patients with multiple sclerosis: comparison of 1.5 T and 7 T. *AJNR. Am. J. Neuroradiol.* 30, 699–702.
- Kurtzke, J.F., 1983. Rating neurologic impairment in multiple sclerosis: an expanded disability status scale (EDSS). *Neurology* 33, 1444–1452.
- Kutzelnigg, A., Lassmann, H., 2006. Cortical demyelination in multiple sclerosis: a substrate for cognitive deficits? *J. Neurol. Sci.* 245, 123–126.
- Lassmann, H., 2008. The pathologic substrate of magnetic resonance alterations in multiple sclerosis. *Neuroimaging Clin NA* 18, 563–576.
- Li, D.K.B., Held, U., Petkau, J., Daumer, M., Barkhof, F., Fazekas, F., Frank, J.A., Kappos, L., Miller, D.H., Simon, J.H., Wolinsky, J.S., Filippi, M., Research, S.L.C.f.M., 2006. MRI T2 lesion burden in multiple sclerosis: a plateauing relationship with clinical disability. *Neurology* 66, 1384–1389.
- Lublin, F.D., Reingold, S.C., 1996. Defining the clinical course of multiple sclerosis: results of an international survey. National Multiple Sclerosis Society (USA) Advisory Committee on Clinical Trials of New Agents in Multiple Sclerosis. *Neurology* 46, 907–911.
- Magliozzi, R., Howell, O., Vora, A., Serafini, B., Nicholas, R., Puopolo, M., Reynolds, R., Aloisi, F., 2007. Meningeal B-cell follicles in secondary progressive multiple sclerosis associate with early onset of disease and severe cortical pathology. *Brain* 130, 1089–1104.
- Mainero, C., De Stefano, N., Iannucci, G., Sormani, M.P., Guidi, L., Federico, A., Bartolozzi, M.L., Comi, G., Filippi, M., 2001. Correlates of MS disability assessed in vivo using aggregates of MR quantities. *Neurology* 56, 1331–1334.
- Mainero, C., Benner, T., Radding, A., van der Kouwe, A., Jensen, R., Rosen, B., Kinkel, R., 2009. In vivo imaging of cortical pathology in multiple sclerosis using ultra-high field MRI. *Neurology* 73, 941.
- Mainero, C., Cohen-Adad, J., Greve, D.N., Benner, T., Radding, A., Fischl, B., Kinkel, R.P., Rosen, B.R., 2010. Subpial pathology as a substrate for cortical thinning in multiple sclerosis: a 7 T MRI study. Proceedings of the 16th Annual Meeting of OHBM, Barcelona, Spain, 3664.
- Metcalf, M., Xu, D., Okuda, D.T., Carvajal, L., Srinivasan, R., Kelley, D.A.C., Mukherjee, P., Nelson, S.J., Vigneron, D.B., Pelletier, D., 2010. High-resolution phased-array MRI of the human brain at 7 Tesla: initial experience in multiple sclerosis patients. *J. Neuroimaging* 20, 141–147.
- Miller, D.H., Barkhof, F., Frank, J.A., Parker, G.J.M., Thompson, A.J., 2002. Measurement of atrophy in multiple sclerosis: pathological basis, methodological aspects and clinical relevance. *Brain* 125, 1676–1695.
- Neema, M., Stankiewicz, J., Arora, A., Dandamudi, V.S., Batt, C.E., Guss, Z.D., Al-Sabbagh, A., Bakshi, R., 2007a. T1- and T2-based MRI measures of diffuse gray matter and white matter damage in patients with multiple sclerosis. *J. Neuroimaging* 17 (Suppl. 1), 16S–21S.
- Neema, M., Stankiewicz, J., Arora, A., Guss, Z.D., Bakshi, R., 2007b. MRI in multiple sclerosis: what's inside the toolbox? *Neurotherapeutics* 4, 602–617.
- Peterson, J.W., Bö, L., Mörk, S., Chang, A., Trapp, B.D., 2001. Transected neurites, apoptotic neurons, and reduced inflammation in cortical multiple sclerosis lesions. *Ann. Neurol.* 50, 389–400.
- Pirko, I., Lucchinetti, C.F., Srinivasan, R., Bakshi, R., 2007. Gray matter involvement in multiple sclerosis. *Neurology* 68, 634–642.
- Pitt, D., Boster, A., Pei, W., Wohleb, E., Jasne, A., Zachariah, C.R., Rammohan, K., Knopp, M.V., Schmalbrock, P., 2010. Imaging cortical lesions in multiple sclerosis with ultra-high-field magnetic resonance imaging. *Arch. Neurol.* 67, 812–818.
- Poonawalla, A.H., Hasan, K.M., Gupta, R.K., Ahn, C.W., Nelson, F., Wolinsky, J.S., Narayana, P.A., 2008. Diffusion-tensor MR imaging of cortical lesions in multiple sclerosis: initial findings. *Radiology* 246, 880–886.
- Pulizzi, A., Rovaris, M., Judica, E., Sormani, M.P., Martinelli, V., Comi, G., Filippi, M., 2007. Determinants of disability in multiple sclerosis at various disease stages: a multiparametric magnetic resonance study. *Arch. Neurol.* 64, 1163–1168.
- Sailer, M., Fischl, B., Salat, D., Tempelmann, C., Schonfeld, M.A., Busa, E., Bodammer, N., Heinze, H.J., Dale, A., 2003. Focal thinning of the cerebral cortex in multiple sclerosis. *Brain* 126, 1734–1744.
- Sanfilippo, M.P., Benedict, R.H.B., Sharma, J., Weinstock-Guttman, B., Bakshi, R., 2005. The relationship between whole brain volume and disability in multiple sclerosis: a comparison of normalized gray vs. white matter with misclassification correction. *Neuroimage* 26, 1068–1077.
- Schmierer, K., Parkes, H.G., So, P.-W., An, S.F., Brandner, S., Ordidge, R.J., Yousry, T.A., Miller, D.H., 2010. High field (9.4 Tesla) magnetic resonance imaging of cortical grey matter lesions in multiple sclerosis. *Brain* 133, 858–867.
- Sled, J.G., Zijdenbos, A.P., Evans, A.C., 1998. A nonparametric method for automatic correction of intensity nonuniformity in MRI data. *IEEE Trans. Med. Imaging* 17, 87–97.
- Stadelmann, C., Albert, M., Wegner, C., Bruck, W., 2008. Cortical pathology in multiple sclerosis. *Curr. Opin. Neurol.* 21, 229–234.
- Tardif, C.L., Collins, D.L., Eskildsen, S.F., Richardson, J.B., Pike, G.B., 2010. Segmentation of cortical MS lesions on MRI using automated laminar profile shape analysis. Medical image computing and computer-assisted intervention. MICCAI International Conference on Medical Image Computing and Computer-Assisted Intervention 13 (Pt 3), 181–188.
- Tedeschi, G., Lavorgna, L., Russo, P., Prinster, A., Dinacci, D., Savettieri, G., Quattrone, A., Livrea, P., Messina, C., Reggio, A., Bresciamorra, V., Orefice, G., Paciello, M., Brunetti, A., Coniglio, G., Bonavita, S., Di Costanzo, A., Bellacosa, A., Valentino, P., Quarantelli, M., Patti, F., Salemi, G., Cammarata, E., Simone, I.L., Salvatore, M., Bonavita, V., Alfano, B., 2005. Brain atrophy and lesion load in a large population of patients with multiple sclerosis. *Neurology* 65, 280–285.
- Tjoa, C.W., Benedict, R.H., Weinstock-Guttman, B., Fabiano, A.J., Bakshi, R., 2005. MRI T2 hypointensity of the dentate nucleus is related to ambulatory impairment in multiple sclerosis. *J. Neurol. Sci.* 234, 17–24.
- van der Kouwe, A.J., Benner, T., Salat, D.H., Fischl, B., 2008. Brain morphometry with multiecho MPRAGE. *Neuroimage* 40, 559–569.
- Wiggins, G.C., Triantafyllou, C., Potthast, A., Reykowski, A., Nittka, M., Wald, L.L., 2006. 32-channel 3 Tesla receive-only phased-array head coil with soccer-ball element geometry. *Magn. Reson. Med.* 56, 216–223.